ARTICLES
PUBLISHED ONLINE: 2 FEBRUARY 2014 | DOI: 10.1038/NCHEM.1857
nature chemistry

Observation of the isotope effect in sub-kelvin reactions

Etay Lavert-Ofir[1†], Yuval Shagam[1†], Alon B. Henson[1], Sasha Gersten[1], Jacek Kłos[2], Piotr S. Żuchowski[3], Julia Narevicius[1] and Edvardas Narevicius[1]*

Quantum phenomena in the translational motion of reactants, which are usually negligible at room temperature, can dominate reaction dynamics at low temperatures. In such cold conditions, even the weak centrifugal force is enough to create a potential barrier that keeps reactants separated. However, reactions may still proceed through tunnelling because, at low temperatures, wave-like properties become important. At certain de Broglie wavelengths, the colliding particles can become trapped in long-lived metastable scattering states, leading to sharp increases in the total reaction rate. Here, we show that these metastable states are responsible for a dramatic, order-of-magnitude-strong, quantum kinetic isotope effect by measuring the absolute Penning ionization reaction rates between hydrogen isotopologues and metastable helium down to 0.01 K. We demonstrate that measurements of a single isotope are insufficient to constrain *ab initio* calculations, making the kinetic isotope effect in the cold regime necessary to remove ambiguity among possible potential energy surfaces.

Many processes in nature exhibit a strong dependence on isotopic composition. Following the discovery of deuterium in the 1930s[1,2], Harold Urey and his colleagues realized that heavier isotope substitution reduces reaction rates, enabling the enrichment of heavy water[3]. At room temperature, this effect has been extensively explored and has become a standard tool in reaction dynamics studies[4]. In striking contrast, the cold regime is dominated by quantum effects in the translational motion of reactants, as has been observed recently in several experiments[5–8]. Until now, the isotope effect has not been observed in low-energy collisions, where it is relevant to the isotopic composition of interstellar clouds[9–11].

In cold chemistry, barrierless reactions play the most important role and usually include highly reactive species such as radicals, ions or excited-state atoms[6] and molecules[12]. The absolute rate in these reactions can be estimated using classical theory that takes into account only the attractive long-range part of the interaction potential between colliding particles. This classical approach for reactions involving hydrogen and deuterium predicts that reaction rates would vary by less than 30%. However, such treatment does not include quantum phenomena, such as the formation of scattering resonances—metastable collisional states that fundamentally change the reactive process and give rise to a dramatic isotope effect in the absolute reaction rate.

In quantum scattering, a state describing a collision that possesses a well-defined angular momentum l is often referred to as a partial wave. The evolution of this state is fully governed by the radial Schrödinger equation given in equation (1),

$$H = \frac{-\hbar^2}{2\mu R}\frac{\partial^2}{\partial R^2}R + V(R) + \frac{\hbar^2 l(l+1)}{2\mu R^2} \qquad (1)$$

where all of the information about the reaction dynamics is included in the reactants' interaction potential $V(R)$, where R is the internuclear distance. The angular momentum is responsible for the additional repulsive term in equation (1) that scales as $\hbar^2 l(l+1)$, the inverse of the square of internuclear distance R, and the inverse of the reduced mass μ. This term modifies the attractive, long-range part of the potential $V(R)$ and produces a potential barrier as shown in Fig. 1c. Under 1 mK, only the 'head-on' collisions with zero angular momentum ($l = 0$) contribute to reactions and the reaction rate assumes a constant value[13,14]. Extracting information about the global interaction potentials in this ultracold regime is thus very challenging. This process is also complicated in the 'warm' collision regime where many angular momentum states contribute to the scattering process and one must observe the differential cross-sections (DCSs), or angle-dependent scattering, including angular distributions or correlation measurements[15], in order to untangle the reaction dynamics. In this regime, the isotope effect has been used in collisional spectroscopy in the observation of a resonance-mediated step-like feature in the isotopic branching ratio of F + HD collisions[16,17]. The scattering resonance was fully resolved later by measuring the DCSs in forward-scattered DCSs of F + H_2 (ref. 18) and backward-scattered DCSs of F + HD (ref. 19). In another development, state-to-state molecular collision cross-sections have been measured on an absolute scale, facilitating comparison with theory[20].

Between the ultracold and 'warm' collision ranges lies the elusive scattering resonance-dominated regime, where single angular momentum states become resolved, in the temperature range from a few millikelvin up to several degrees kelvin. At these temperatures the colliding particles' de Broglie wavelength is an order of magnitude larger than the molecular dimensions, and particles may tunnel through the barrier created by centrifugal repulsion. At a certain de Broglie wavelength or collision energy, a metastable scattering state is formed. The resonance wavefunction of this metastable state is strongly localized between the inner turning point, where the particle separation is minimal, and the position of the centrifugal barrier, as shown in Fig. 1a. This is in a stark contrast to the continuum scattering wavefunction shown in Fig. 1b, which

[1]Department of Chemical Physics, Weizmann Institute of Science, Rehovot 76100, Israel, [2]Department of Chemistry and Biochemistry, University of Maryland, College Park, Maryland 20742-2021, USA, [3]Institute of Physics, Nicolaus Copernicus University, Grudziądzka 5, 87-100 Toruń, Poland; †These authors contributed equally to this work. *e-mail: edn@weizmann.ac.il

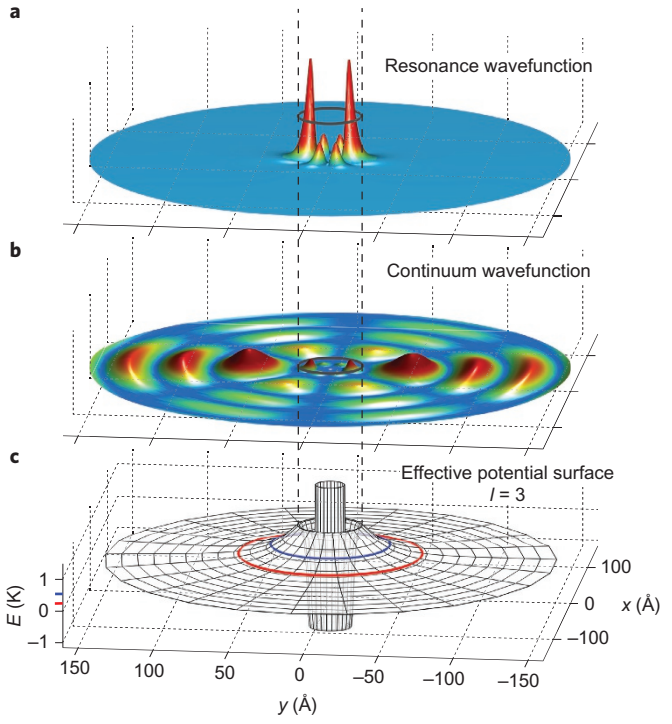

Figure 1 | Plot of effective potential surface and wavefunctions at different energies. a–c, The two-dimensional effective potential surface of the collision pair He^*–H_2 for the partial wave $l = 3$ (**c**) and numerically solved wavefunction probability densities ($|\psi(\vec{R})|^2$) for this potential surface at different energies (**a**,**b**). The radial part of the wavefunction is multiplied by the corresponding partial wave spherical harmonic function and plotted as a function of the intermolecular distance and the collision angle. The corresponding collision energies in **a** and **b** are above the dissociation threshold, but below the centrifugal barrier height. The collision energy of the wavefunction in **a** is at the scattering resonance energy of 0.23 K, as indicated by the red tick mark and circle in **c**. Here the colliding particle tunnels through the centrifugal barrier leading to a highly localized wavefunction within the confines of the potential well. In **b**, the probability density of the continuum wavefunction is shown, scaled up by a factor of 30 compared with **a**. The collision energy in this case is far away from the resonance energy at 0.51 K, as indicated by the blue tick mark and circle in **c**. The colliding particle is unable to tunnel through the centrifugal barrier effectively, so the resulting probability density is mostly situated on the outer side of the barrier where the reaction is much less likely to occur. The resonance wavefunction (**a**) is therefore far more likely to react than the continuum wavefunction (**b**). The scattering resonance leads to the domination of the scattering process by a single partial wave over the background partial waves.

has only a small fraction of the probability amplitude localized behind the centrifugal barrier. Due to the much higher probability of finding particles at short separations in the resonance state, a dramatic increase in the absolute reaction rate can be observed. Importantly, scattering resonances span the short-range interaction region as well as the long-range attractive part of the potential energy surface. This makes scattering resonances a perfect probe for the interaction potential if they can be resolved in an experiment where the collision energy can be continuously tuned. This is similar to vibrational spectroscopy where transitions between vibrational states are detected using a tunable radiation source. Calculating the energy positions of the scattering resonances is in principle possible using *ab initio* potential energy surfaces. However, the small inaccuracies that exist even in state-of-the-art *ab initio* methods may lead to variations by orders of magnitude in the

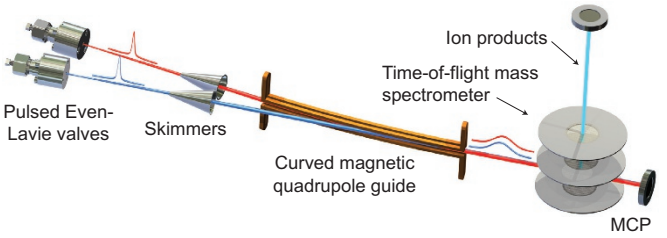

Figure 2 | Schematic of the merged supersonic beam configuration. Two supersonic beams are produced by pulsed Even–Lavie valves[29], which are followed by skimmers. The red beam, which consists of paramagnetic metastable helium, is merged with the blue beam, which consists of hydrogen isotopologues, by a magnetic quadrupole guide. The beams are characterized with an on-axis MCP and a TOF-MS positioned perpendicular to the propagation direction. The ion products of the Penning ionization reactions (light blue) are detected with a TOF-MS with the ionization element turned off.

reaction rate, due to uncertainty in the energy of a particular resonance state[21,22]. Collisional spectroscopy, which probes these states directly, serves as a benchmark test for the best available theories.

Although collisional spectroscopy is very sensitive to the vibrational structure of the potential, this structure does not necessarily correspond to a unique interaction potential surface. We will show that utilizing the isotope effect in collisional spectroscopy can remove the ambiguity among the different interaction potential surfaces, which predict similar vibrational structures. In conventional vibrational spectroscopy the isotope effect modifies the kinetic term in the Hamiltonian, which leads to a shift in the vibrational levels, thus enabling a more sensitive and selective probe of the molecular structure. In collisional spectroscopy the centrifugal repulsion term is also modified by changes in the reduced mass, as can be seen in equation (1). To study the isotope effect in cold chemistry reactions, we measured the Penning ionization reaction rates for collisions between metastable helium, ^4He (2^3S), which we denote He^*, and the hydrogen isotopologues H_2, HD and D_2. The reduced masses of the colliding pairs are 1.34, 1.72 and 2.01 AMU, respectively. Penning ionization is a fundamental process in nature in which a neutral particle is ionized upon collision with another particle in an excited electronic state[23], as described by equation (2),

$$A^* + M \rightarrow A + M^+ + e^- \quad (2)$$

where A and M are neutral particles and the superscript * denotes the excited electronic state. The effect of the increase in reduced mass is twofold. First, it lowers the centrifugal term in the effective potential, reducing the height of the centrifugal barrier and increasing the depth of the potential well. Second, due to the change in the kinetic term in the system Hamiltonian, the quasi-bound states are shifted to lower energies with respect to the centrifugal barrier. As a result, the resonance states for each system appear at different collision energies. This effect gives rise to the quantum kinetic isotope effect (QKIE), which is ubiquitous in cold chemistry reactions. In contrast to the conventional KIE, the quantum counterpart depends on the collision energy. We demonstrate that QKIE can increase the total reaction rate by up to an order of magnitude without dependence on mass scaling. The relative energies of quantum scattering states for different isotopologues determine the magnitude and direction of the effect, as we will show in the following.

Results and discussion

We used our merged supersonic beam configuration[6] with a time-of-flight mass spectrometer (TOF-MS)[24] (Fig. 2) to measure the

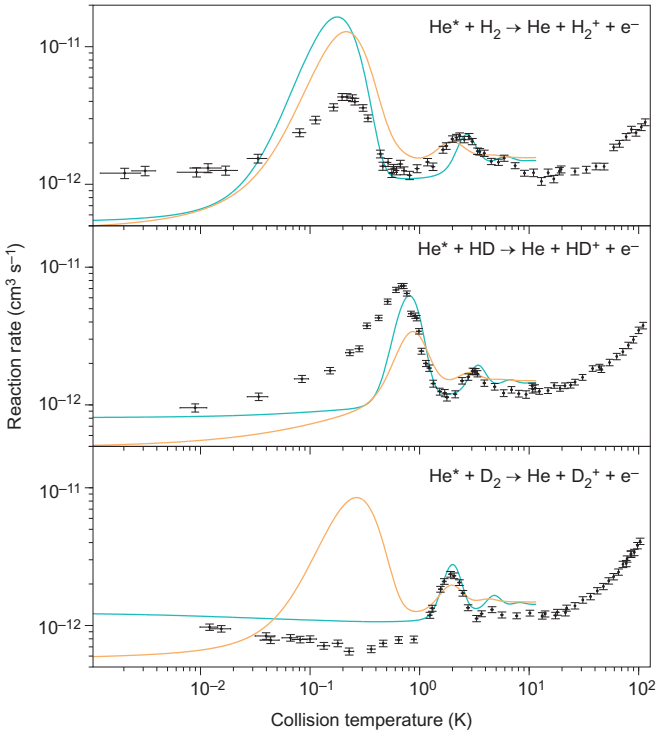

Figure 3 | Penning ionization reaction rates of metastable helium, He*(2^3S) and the hydrogen isotopologues H_2, HD and D_2. The reaction rates are depicted by black points as a function of collision temperature. The energy positions of the scattering resonances shift according to the reduced mass of the colliding particles. The plotted curves indicate the theoretical reaction rates derived from the scaled coupled cluster potential[26] with scaling factors of $\lambda = 0.74$ (orange) and $\lambda = 1.15$ (cyan). When observing the H_2 rate alone, it is not clear which of the scaling options provides the best agreement in terms of peak positions. Only when all three isotopologues are taken into account does the $\lambda = 1.15$ scaling option show indisputably better agreement. Error bars indicate the standard error in the reaction rate and the collision energy, calculated according to 150–300 measurements per data point. The He*–H_2 reaction that was originally observed in Henson *et al.*[6] has been re-measured with the configuration described in the Methods.

Penning ionization reaction rates of metastable helium with the different hydrogen isotopologues. These reaction rates are shown in Fig. 3. Clearly resolved scattering resonances appear in all three systems, with shifted energy positions. The measurements show a very strong kinetic isotope effect, observed in the total reaction rate in the collision temperature range from 10 mK up to 100 K. Interestingly, at the collision temperature of 0.7 K, the He*–HD reaction exhibits a very strong kinetic isotope effect, simultaneously proceeding an order of magnitude faster than the lighter He*–H_2 reaction and the heavier He*–D_2 reaction. If the reaction rate would simply scale inversely with the reactants' relative velocity, as described by semiclassical Penning ionization reaction theory[25], then the reaction with the H_2 molecule would be no more than 10% and 20% slower than the reaction with the heavier HD and D_2 molecules, respectively. This behaviour reflects the dramatic effect that scattering resonances have on the total reaction rate.

We calculated the reaction rates of the three systems according to the latest state-of-the-art *ab initio* interaction potential derived using coupled cluster theory[26], in the same manner as in the work by Henson and colleagues[6]. Because the centre of mass is shifted in the case of He*–HD, we needed to re-expand the potential surface in the shifted coordinate system[27], yielding a subpercent reduction in the depth of the isotropic potential.

The numerical value of the interaction potential at any given coordinate was scaled by a factor λ in order to test how accurately the resonance positions are reproduced by calculations using the *ab initio* potential. This sensitivity analysis is routinely used in theoretical investigations of low-temperature scattering phenomena[21,22,27,28]. Given the extreme sensitivity of reaction rates toward the positions of scattering resonances, this analysis provides a very convenient basis for comparison of theory with experiment. Figure 4 shows the calculated reaction rate for the He*–H_2 reaction at 0.23 K, the collision energy where the strongest resonance appears in our measurements, as a function of the scaling parameter. The analysis reveals two options, with scaling factors of 1.15 and 0.74, showing reasonable agreement with the experimental data in terms of the position of the major resonance peak. The asterisks in Fig. 4 mark the values of λ for which both major and minor peaks have the best overall agreement. Both of the corresponding calculated reaction rates of the He*–H_2 collision pair are presented in Fig. 3 and do not show a clear preference in the choice of potential surface. The uncertainty is only removed once the theoretical reaction rate for all three collision pairs is compared to the experimental results. An additional resonance appears in the theoretical reaction rate for the He*–D_2 collision pair at low energies, which does not exist in the experimental results, disqualifying the shallower potential with the $\lambda = 0.74$ scaling option.

The major peak in the reaction rate calculated according to the unscaled *ab initio* potential ($\lambda = 1$) is located at 1.16 K, which is almost an order of magnitude away from the observed energy of the peak at 0.23 K. The sensitivity analysis (Fig. 4) clearly shows that this peak is virtually nonexistent for this scaling value as it falls directly between the two peaks. By scaling the potential by a mere 15% we are able to guide the theoretical *ab initio* calculation to agree with the experimental results. Such a change to the potential is within the expected error bound of the methodology used to obtain the potential energy surface (see the discussion in the Supplementary Information). According to the potential with the deeper well corresponding to the $\lambda = 1.15$ scaling option, we find that each of the scattering resonances observed in the reaction rates is formed by a single partial wave, which dominates over the background. The corresponding partial wave of the respective major and minor resonances is $l = 3, 4$ for H_2, $l = 4, 5$ for HD and $l = 5, 6$ for D_2.

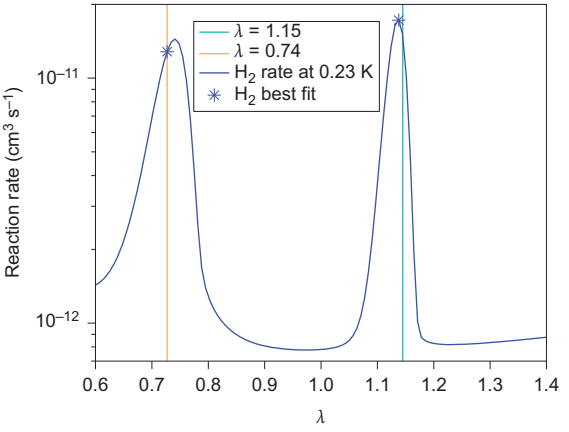

Figure 4 | Sensitivity analysis of the He*–H_2 reaction. The theoretical reaction rate at 0.23 K for the He*–H_2 system is plotted as a function of λ, the scaling factor of the potential (blue curve). This energy corresponds to the observed position of the strongest scattering resonance observed in this system. Asterisks indicate the values of λ with the closest agreement in terms of peak position for both the major and minor observed peaks in the reaction rate. The vertical lines indicate two values of λ for which the energy-dependent reaction rate is plotted in Fig. 3.

We have shown that collisional spectroscopy of scattering resonances combined with the isotope effect serves as a sensitive tool to probe vibrational structures and remove the uncertainty in the potential surface of collision pairs.

Methods

Experimental configuration and analysis. The experimental configuration consists of two supersonic molecular beams formed by pulsed Even–Lavie valves[29] in a merged beam apparatus[6] (Fig. 2). One beam consists of ^{4}He and is excited to the 2^3S metastable state (He*) with a dielectric barrier discharge[30] located immediately after the valve. This beam is merged using a magnetic quadrupole guide with a straight beam, which consists of different isotopologues of H_2. The velocity of the straight beam is tuned by changing the valve temperature as well as seeding the isotopologues in noble carrier gas mixtures, while the He* beam velocity is fixed at 870 m s^{-1}. In this manner, the collision temperature was tuned from 100 K down to 10 mK.

The He* beam was characterized with an on-axis multichannel plate (MCP). The straight beam was characterized with a home-built TOF-MS[24] positioned perpendicular to the line of propagation. To obtain the longitudinal profile of the hydrogen isotopologues we operated the TOF-MS in a multipulsed mode, with the ionization element turned on, while the beam travelled through the ion collection volume of the TOF-MS. Each pulse forms a 7 μs integrated portion of the beam, constructing a beam profile of time bins. The product ions of the reaction were also measured by the TOF-MS but with the ionization element turned off. The three bins at the centre of the neutral beam profile were summed for both the product ions and the hydrogen isotopologue reactants. This sum for the product ions was divided by the sum of the hydrogen isotopologue signal as well as the area of the He* beam at the appropriate time interval to give the overall unitless reaction rate. The absolute numbers for the reaction rates were calculated by normalizing the unitless results of the He*–H_2 reaction, which were re-measured in this set-up, according to the results at higher collision energies provided by Henson and colleagues[6].

Because the opening duration of the Even–Lavie valve[29] is short compared to the time-of-flight, the supersonic beams develop a correlation in phase-space, reducing the local velocity spread[31]. As such, the collision energies of this time-sliced detection configuration, taking into account the phase-space correlation effect, were calculated according to the work by Shagam and Narevicius[31]. The hydrogen isotopologue beams are neat and very cold (<1 K), so the molecules are in the ground state. The resulting *ortho*-hydrogen to *para*-hydrogen ratio is 3:1 (refs 8,32).

Calculation details. The He*–H_2 potential was calculated with the supermolecular approach using restricted Hartree–Fock calculations, which ensures the proper orbital occupation pattern corresponding to the ^{3}S excited state of the helium atom, which is described in detail by Hapka and colleagues[26], and followed by a spin-unrestricted coupled cluster with single and double excitation with a perturbative correction for the triple excitation, UCCSD(T).

The reaction rate was calculated by adding an imaginary decay term to the potential surface, as described in the Penning ionization review by Siska[25].

Received 13 September 2013; accepted 17 December 2013; published online 2 February 2014

References

1. Urey, H., Brickwedde, F. & Murphy, G. A hydrogen isotope of mass 2. *Phys. Rev.* **39,** 164–165 (1932).
2. Urey, H., Brickwedde, F. & Murphy, G. A hydrogen isotope of mass 2 and its concentration. *Phys. Rev.* **40,** 1–15 (1932).
3. Washburn, E. W. & Urey, H. C. Concentration of the H^2 isotope of hydrogen by the fractional electrolysis of water. *Proc. Natl Acad. Sci. USA* **18,** 496–498 (1932).
4. Westheimer, F. H. The magnitude of the primary kinetic isotope effect for compounds of hydrogen and deuterium. *Chem. Rev.* **61,** 265–273 (1961).
5. Ospelkaus, S. *et al.* Quantum-state controlled chemical reactions of ultracold potassium–rubidium molecules. *Science* **327,** 853–857 (2010).
6. Henson, A. B., Gersten, S., Shagam, Y., Narevicius, J. & Narevicius, E. Observation of resonances in Penning ionization reactions at sub-kelvin temperatures in merged beams. *Science* **338,** 234–238 (2012).
7. Ni, K-K. *et al.* Dipolar collisions of polar molecules in the quantum regime. *Nature* **464,** 1324–1328 (2010).
8. Chefdeville, S. *et al.* Observation of partial wave resonances in low-energy O_2–H_2 inelastic collisions. *Science* **341,** 1094–1096 (2013).
9. Millar, T. J. Deuterium fractionation in interstellar clouds. *Space Sci. Rev.* **106,** 73–86 (2003).
10. Millar, T. J., Bennett, A. & Herbst, E. Deuterium fractionation in dense interstellar clouds. *Astrophys. J.* **340,** 906 (1989).
11. Messenger, S. Identification of molecular-cloud material in interplanetary dust particles. *Nature* **404,** 968–971 (2000).
12. Bell, M. T., Bell, P. & Softley, T. Ultracold molecules and ultracold chemistry. *Mol. Phys.* **107,** 99–132 (2009).
13. Wigner, E. On the behavior of cross sections near thresholds. *Phys. Rev.* **73,** 1002–1009 (1948).
14. Krems, R. V. Molecules near absolute zero and external field control of atomic and molecular dynamics. *Int. Rev. Phys. Chem.* **24,** 99–118 (2005).
15. Herschbach, D. Molecular collisions, from warm to ultracold. *Faraday Discuss.* **142,** 9 (2009).
16. Skodje, R. T. *et al.* Observation of a transition state resonance in the integral cross section of the F + HD reaction. *J. Chem. Phys.* **112,** 4536 (2000).
17. Skodje, R. *et al.* Resonance-mediated chemical reaction: F + HD→HF + D. *Phys. Rev. Lett.* **85,** 1206–1209 (2000).
18. Qiu, M. *et al.* Observation of Feshbach resonances in the F + H_2→HF + H reaction. *Science* **311,** 1440–1443 (2006).
19. Ren, Z. *et al.* Probing the resonance potential in the F atom reaction with hydrogen deuteride with spectroscopic accuracy. *Proc. Natl Acad. Sci. USA* **105,** 12662–12666 (2008).
20. Kirste, M. *et al.* Quantum-state resolved bimolecular collisions of velocity-controlled OH with NO radicals. *Science* **338,** 1060–1063 (2012).
21. Janssen, L. M. C., van der Avoird, A. & Groenenboom, G. C. Quantum reactive scattering of ultracold NH($X^3\Sigma^-$) radicals in a magnetic trap. *Phys. Rev. Lett.* **110,** 063201 (2013).
22. Janssen, L. M. C., Żuchowski, P. S., van der Avoird, A., Hutson, J. M. & Groenenboom, G. C. Cold and ultracold NH–NH collisions: the field-free case. *J. Chem. Phys.* **134,** 124309 (2011).
23. Druyvesteyn, M. & Penning, F. The mechanism of electrical discharges in gases of low pressure. *Rev. Mod. Phys.* **12,** 87–174 (1940).
24. Wiley, W. C. & McLaren, I. H. Time-of-flight mass spectrometer with improved resolution. *Rev. Sci. Instrum.* **26,** 1150 (1955).
25. Siska, P. E. Molecular-beam studies of Penning ionization. *Rev. Mod. Phys.* **65,** 337–412 (1993).
26. Hapka, M., Chałasiński, G., Kłos, J. & Żuchowski, P. S. First-principle interaction potentials for metastable He(^{3}S) and Ne(^{3}P) with closed-shell molecules: application to Penning-ionizing systems. *J. Chem. Phys.* **139,** 014307 (2013).
27. Żuchowski, P. & Hutson, J. Low-energy collisions of NH_3 and ND_3 with ultracold Rb atoms. *Phys. Rev. A* **79,** 062708 (2009).
28. Janssen, L. M. C., Żuchowski, P. S., van der Avoird, A., Groenenboom, G. C. & Hutson, J. M. Cold and ultracold NH–NH collisions in magnetic fields. *Phys. Rev. A* **83,** 022713 (2011).
29. Even, U., Jortner, J., Noy, D., Lavie, N. & Cossart-Magos, C. Cooling of large molecules below 1 K and He clusters formation. *J. Chem. Phys.* **112,** 8068 (2000).
30. Luria, K., Lavie, N. & Even, U. Dielectric barrier discharge source for supersonic beams. *Rev. Sci. Instrum.* **80,** 104102 (2009).
31. Shagam, Y. & Narevicius, E. Sub-kelvin collision temperatures in merged neutral beams by correlation in phase-space. *J. Phys. Chem. C* **117,** 22454–22461 (2013).
32. Chefdeville, S. *et al.* Appearance of low energy resonances in CO–*para*-H_2 inelastic collisions. *Phys. Rev. Lett.* **109,** 1–5 (2012).

Acknowledgements

The authors thank U. Even and Y. Prior for discussions. The authors thank J.W. Rosenberg for reading the manuscript. This research was made possible, in part, by the historic generosity of the Harold Perlman family. E.N. acknowledges support from the Israel Science Foundation and the Minerva Foundation. J.K. acknowledges financial support through the United States National Science Foundation (grant no. CHE-1213332) to M. Alexander. P.S.Z. was supported by the Iuventus Plus grant by the Polish Ministry of Science and Higher Education.

Author contributions

The experimental work and data analysis were carried out by E.L-O., Y.S., A.B.H., S.G., J.N. and E.N. The *ab initio* potential surfaces were calculated by J.K. and P.S.Z.

Additional information

Supplementary information is available in the online version of the paper. Reprints and permissions information is available online at www.nature.com/reprints. Correspondence and requests for materials should be addressed to E.N.

Competing financial interests

The authors declare no competing financial interests.